ISSN 1063-7834, Physics of the Solid State, 2021, Vol. 63, No. 1, pp. 84–89. © Pleiades Publishing, Ltd., 2021.
Russian Text © The Author(s), 2021, published in Fizika Tverdogo Tela, 2021, Vol. 63, No. 1, pp. 85–90.

SEMICONDUCTORS

Distribution of Misfit Dislocations and Elastic Mechanical Stresses in Metamorphic Buffer InAlAs Layers of Various Constructions

D. B. Pobat[a], *, V. A. Solov'ev[a], M. Yu. Chernov[a], and S. V. Ivanov[a]

[a] *Ioffe Institute, St. Petersburg, 194021 Russia*

**e-mail: pobat.dima@gmail.com*

Received September 18, 2020; revised September 18, 2020; accepted September 19, 2020

Abstract—The equilibrium distributions of the misfit dislocation density $\rho(z)$ and elastic stresses $\varepsilon(z)$ are calculated along the direction of the epitaxial growth of the metamorphic InAlAs/GaAs(001) layer with higher In content (to 87 mol %) and various profiles of varying the composition: step, linear, and root. The calculations are performed using the method based on iteration searching for the minimum total energy of the system. It is shown that the largest differences between various constructions of the buffer layer are observed in the character of distributions $\rho(z)$, rather than $\varepsilon(z)$. Unlike the traditional constructions with a step and linear gradients of the composition, which are characterized by a quite homogeneous distribution of misfit dislocations, in a buffer layer with a root composition gradient, the main part of such dislocations is concentrated in the lower part of the layer near the heteroboundary with a GaAs substrate, and their density sharply decreases by more than one order of value along the layer thickness, achieving the value minimum for all abovementioned constructions. In spite of the fact that the important effect of interacting the dislocations to each other is not taken into account in this work, the calculations enable us to establish the main peculiarities of the distributions $\rho(z)$ and $\varepsilon(z)$ in various metamorphic buffer InAlAs layers, which were observed experimentally before. Thus, this approach can be effectively used when designing optimal constructions of the device metamorphic heterostructures.

Keywords: misfit dislocations, elastic stresses, metamorphic heterostructures, InAlAs/GaAs, large lattice misfit

DOI: 10.1134/S1063783421010170

1. INTRODUCTION

The use of semiconductor heterostructures based on $In_x(Al, Ga)_{1-x}As$ solid solutions with high In content ($x \geq 0.7$) enables one to design high-efficient devices of modern electronics including high electron mobility transistors [1], heterojunction bipolar transistors [2], and also semiconductor light-emitting diodes and mid-infrared lasers radiating in a middle IR range (2–5 μm) [3, 4]. It is interesting to realize similar structures on GaAs substrates that are characterized by high manufacturability and low cost as compared to those of InSb and GaSb substrates used commonly. However, a large lattice misfit of GaAs substrate (a_s) and the active region (a) $\Delta a/a > 5\%$ leads to the formation of a high misfit dislocation (MD) density and also threading dislocation (TD) density that adversely affect the output parameters of the structures.

One of effective approach for solving this problem is the use of a metamorphic buffer layer (MBL) that is a layer of the solid solution with variable composition, in which the lattice parameter is gradually changed from a_s up to required value during the layer growth. Commonly, MBLs with a step or linear profiles of changing the composition are used [5], and this fact is related to a simplicity of realizing such MBL as metamorphic structures are grown by the molecular-beam epitaxy (MBE) and the possibility of using the complex theory of relaxation of elastic stresses developed in [6, 7] for estimating and controlling the density of dislocations and residual elastic mechanical stresses forming in the structure. The absence of similar theory for nonlinear MBL, along with the complexities of the technical realization of a nonlinear profile of changing the composition, retards their active application in metamorphic structures, although it was shown that the use of $In_xAl_{1-x}As$ MBL with a nonlinear composition gradient and the maximum In content in it $x_{max} > 0.5$, instead of a linear or step MBL, enables one to obtain the TD density lower by an order of value ($\sim 10^7$ cm^{-2}) and also to increase the thickness of so called dislocation-free region (d_{free}) [8, 9]. To understand the processes of the relaxation of elastic stresses and the distribution of MD in MBL with a nonlinear profile of changing the composition, the numerical approach can be quite efficient in spite of the absence

of the theory and small number of the published experimental works [10].

This work is devoted to the modeling the profiles of the distribution of the MD density and elastic stresses along the direction of the epitaxial growth of the $In_xAl_{1-x}As$ (x_{max} = 0.75–0.87) MBL with a linear, step, and root gradients of changing the composition and also to the comparison of the modeling results to the experimental data.

2. CALCULATION OF ELASTIC MECHANICAL STRESSES AND THE MISFIT DISLOCATION DENSITY IN MBL

In this work, the equilibrium profiles of the distributions of the elastic stresses and the MD density in the direction of the growth of the studied structures with different types of MBL were calculated using the numerical method described in [10]. This method (the method of successive approximations) is based on the iteration searching for the minimum total energy of the system that includes the elastic energy (E_ε) and the MD energy (E_d). Further we briefly describe the algorithm of searching for the minimum total energy of the system with the removal of some unclearities of its presentation and also errors in writing the final formulas, that we detected in [10].

MBL with summary thickness L is separated into N sublayer each of which has its proper set of the parameters: sublayer thickness h_i, lattice parameter a_i and elastic moduli C_{kl} (Table 1). Taking into account that the calculation accuracy increases as the value of h_i decreases, the number of sublayers N was chosen so that h_i does not exceed 5 nm. The elastic stresses in a layer are determined according to Eq. (1):

$$\varepsilon_i = f_i + \sum_{m=1}^{i} b_i' \rho_i h_i, \qquad (1)$$

where $f_i = (a_s - a_i)/a_i$ is the lattice misfit of sublayer i and substrate, b_i' is the Burgers vector projection on the axis coinciding with the growth direction, and ρ_i is the MD density in sublayer i.

The elastic energy of the system per unit area is

$$E_\varepsilon = \sum_{i=1}^{N} \varepsilon_i^2 Y_i h_i, \qquad (2)$$

where $Y_i = C_{11i} + C_{12i} - 2C_{12i}^2/C_{11i}$ is the Young's modulus in the [001] direction [12]. The formula for the calculation of the dislocation energy per unit area can be written as follows:

Table 1. Parameters of materials studied in this work [11]

Material	a, nm	b, nm	C_{11}, GPa	C_{12}, GPa
GaAs	0.56534	0.400	118.4	53.7
AlAs	0.5611	0.400	120.2	57.0
InAs	0.60584	0.428	83.29	45.26

$$E_d = \sum_{i=1}^{N} \frac{G_i b_i^2 (1 - \nu_i \cos^2\alpha)}{2\pi(1-\nu_i)} \left[\ln\left(\frac{L - \sum_{k=1}^{i-1} h_k}{b_i} \right) + 1 \right] \rho_i h_i, \qquad (3)$$

where α is the angle between the Burgers vector and dislocation line, $G_i = (C_{11i} - G_{12i})/2$ and $\nu_i = C_{12i}/(C_{11i} + C_{12i})$ are the rigidity modulus and the Poisson ratio, respectively [12]. As known, the most characteristic MD in stressed semiconductor A^3B^5 heterostructures with the crystal lattice of the zinc blende type are 60° dislocations [13, 14]. Thus, the value α = 60° was used in our calculations.

As the initial calculation date, we use the initial values and take, for simplicity, $\rho_i = 0$ in each sublayer; in this case $\varepsilon_i = f_i$, which corresponds to the complete absence of the relaxation in the structure. Then, we determine the first iteration value ρ_i^1 for each sublayer i, beginning from the first sublayer. To do this, we consider three values of the "MD density" for a given layer (i): $\rho_i^{up} = \rho_i + \Delta\rho$, $\rho_i^{const} = \rho_i$, and $\rho_i^{down} = \rho_i - \Delta\rho$ and for several neighboring layers (i + 1, i + 2, and so on). For example, in the case of simultaneous consideration of two layers (i and i + 1), the expressions for three values of the "MD density" in the i + 1 layer will have the form: $\rho_{i+1}^{up} = \rho_{i+1} + \Delta\rho$, $\rho_{i+1}^{const} = \rho_{i+1}$, and $\rho_{i+1}^{down} = \rho_{i+1} - \Delta\rho$. Note that the components listed above listed above can be both positive and negative. In this case, the positive values correspond to the case of elastic tensile stresses and the negative, to the compression stresses. Then, according to Eqs. (1)–(3), we calculate the total energy of the system $E_\varepsilon + E_d$ for various combinations of the values of the "MD density" in the considered neighboring layers and we choose the combination that corresponds to the minimum value of $E_\varepsilon + E_d$. The numbers of the combinations in the case of simultaneous consideration of one, two, and three layers are 3, 9, and 27, respectively. Because the calculation using one layer leads to the appearance of nonphysical oscillations in the calculated distribution of the MD density, and although the use of three and more layers insignificantly increases the accuracy of the calculations, but needs substantially larger labor consumptions [10], we use in this work the simultane-

ous consideration of two layers as the most optimal variant.

After the determination of the combinations of corrected values of the "MD density" for layers i and $i + 1$, the first of them is the desired value ρ_i^1, we repeat the procedure described above for the following pair of layers $i + 1$ and $i + 2$. In this case, the corrected value of the "MD density" for layer $i + 1$ obtained during the preceding step was chosen as the initial value for ρ_{i+1}. This procedure is repeated until the first iteration values will be obtained for all sublayers. It should be noted that, as the start value of correction $\Delta\rho$, we choose the value exceeding the maximum possible MD density in the structure under study, corresponding to the case of the complete relaxation of elastic stresses in it (in this case, 10^{12} cm^{-2}).

At the next calculation step, correction $\Delta\rho$ decreases by $\Delta\rho_{step}$ (for example, by 10% from the initial value), and the process is repeated once again for each sublayer, until desired values of ρ_i^2, ρ_i^3, and so on, will be obtained for all sublayers. The calculation process is stopped as the required accuracy $\Delta\rho^f$ (50 cm^{-2}) of determining the MD density is achieved.

3. RESULTS AND DISCUSSION

Using this numerical method, we calculated the equilibrium distributions of the MD density and elastic stresses along the direction of the epitaxial growth for various constructions of $In_xAl_{1-x}As$ both traditional most frequently used in the literature: with step, linear and piece-linear gradients of the composition in the direction of the MBL growth $x(z)$ and for a nonlinear MBL developed recently with root dependence $x(z) = x_i + (x_{max} - x_i)(z/L)^{0.5}$, where x_i and x_{max} are the In contents in the initial and final MBL regions. Figure 1 shows the distribution profiles of the MD density along the depth $\rho(z)$ for the listed MBL; in this case, the layer thickness and also the range of changing the solid solution composition were chosen to be the same for all MBL constructions (L = 1435 nm, x = 0.05–0.87). We considered the step MBL consisting of 12 equal portions, at the boundaries of which the In content was changed by the same value. The piece-linear MBL consisted of two layers with a linear gradient of the composition, whose value was decreased by a factor of 1.5 at the transition from the lower layer to the upper layer at $x = 0.6$, by analogy with [15]. In spite of significant difference in the characters of these distributions, the upper parts of each MBL constructions contain regions in which $\rho = 0$ that corresponds to so called dislocation-free region observed experimentally.

As seen from Fig. 1, distribution $\rho(z)$ for the step MBL (curve *1*) is the alternating of narrow peaks corresponding to the regions, in which a step change in the composition accompanied by the formation of

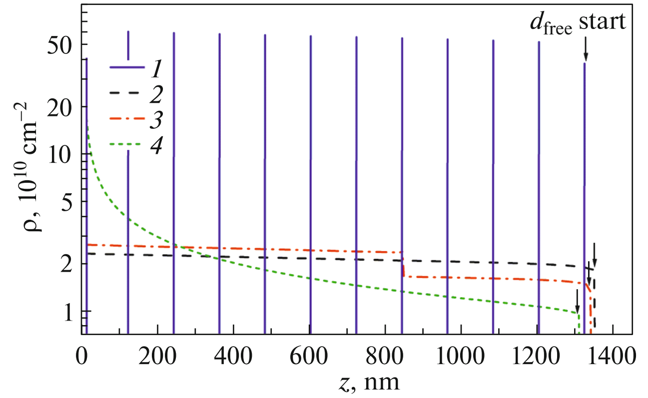

Fig. 1. Calculated coordinate dependences of the MD density along the growth direction obtained for $In_xAl_{1-x}As$ MBL (L = 1435 nm, x = 0.05–0.87) with different profiles of the change in the composition: (*1*) step, (*2*) linear, (*3*) piece–linear, and (*4*) root.

MD takes place, and the portions, in which there are no MD completely; in this case, the latter portion plays a part of the d_{free} region. It also should be noted that the peak values of ρ in this type of MBL are slightly changed in the structure thickness, and ρ achieves value $\rho_0 \sim 4 \times 10^{11}$ cm^{-2} in the upper part of the MBL that is immediately adjacent to the d_{free} region. In the case of MBL with a linear profile, the changes in the MD composition are almost homogeneously distributed over the thickness (curve *2*), and their density slightly decreases as MBL grows, achieving a value of $\rho_0 \sim 2 \times 10^{10}$ cm^{-2} in its upper part; this value is more than one order of value lower than that in the case of the step MBL. The analysis of the piece-linear MBL gives the distribution of the MD density (curve *3*) close in character to the preliminary construction, except for the step change in ρ in the point of decreasing the composition gradient ($x = 0.6$, z = 845 nm) which allows us to reach an insignificant decrease in ρ in the upper part of the piece-linear MBL ($\rho_0 \sim 1.5 \times 10^{10}$ cm^{-2}) as compared to the linear MBL. In the case of the root MBL, the profile of distribution $\rho(z)$ significantly differs from the profiles of other constructions of MBL, which is observed as a nonlinear decrease in the MD density by more than an order of value as the layer grows, and the density achieves the value $\rho_0 \sim 9 \times 10^9$ cm^{-2} in the upper part of MBL. As it is seen from Fig. 1, the distribution profiles $\rho(z)$ for various constructions are strongly different from each other not only in characters, but also in the MD density values in the region immediately adjacent to the d_{free} portion; in this case, the minimum value ρ_0 is achieved in root MBL. This type of MBL is characterized by the largest value d_{free} = 125 nm, while the step, linear, and piece–linear MBLs have d_{free} = 115, 85, and 95 nm, respectively. It should be noted

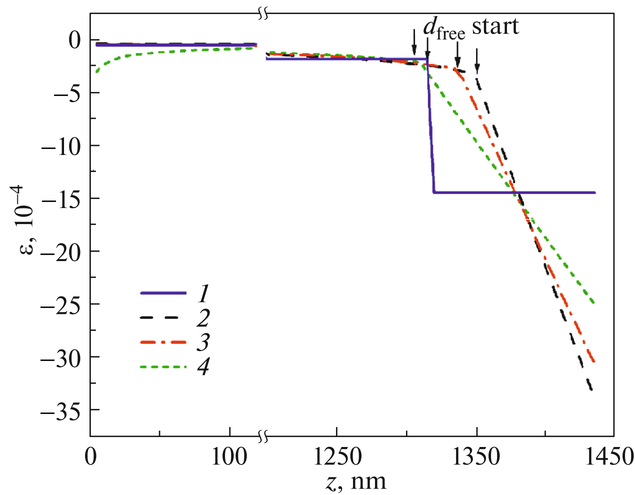

Fig. 2. Calculated coordinate dependences of the MD density along the growth direction obtained for $In_xAl_{1-x}As$ MBL (L = 1435 nm, x = 0.05–0.87) with different profiles of the change in the composition: (*1*) step, (*2*) linear, (*3*) piece–linear, and (*4*) root.

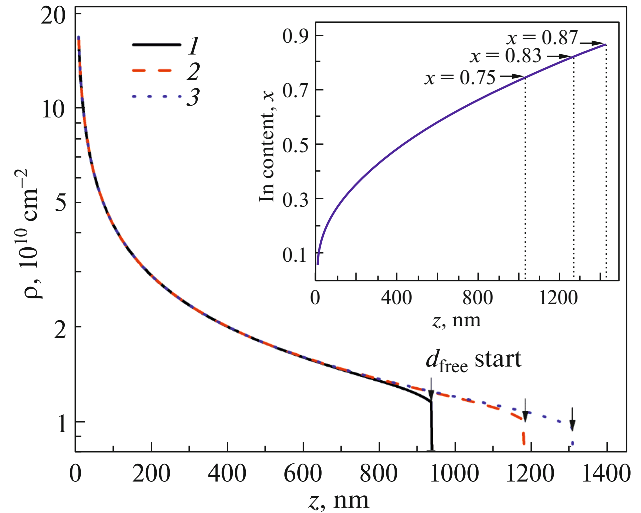

Fig. 3. Calculated coordinate dependences of the MD density along the growth direction obtained for $In_xAl_{1-x}As$ MBL with one root profile of changing the composition at various values of parameters x_{max} and L: (*1*) 0.75 and 1050 nm, (*2*) 0.83 and 1300 nm, and (*3*) 0.87 and 1435 nm. The inset shows the profile of changing in the In content along the layer thickness used in our calculations.

that the found features of the MD density distribution are also observed in the experiment. In [16], the detailed TEM studies were performed for the cross sections of the samples containing MBLs with the root and piece–linear profiles of changing the composition; in that case, the layer thicknesses and the range of varying the In content in the samples had the values close to the parameters considered in this work. The TEM data show that, in MBL with piece–linear profiles of changes in the composition, MD are actually distributed quite homogeneously in the layer thick up to the d_{free} region, while, in the case of a root MBL, the value of ρ significantly decreases along the growth direction. It should be also noted that the significant increase in thickness d_{free} in the root MBL (290 nm) observed experimentally as compared to that of the piece–linear MBL (180 nm) [16] agrees quite well with the data of our calculations that demonstrate the corresponding increase in the value of d_{free} by a factor of more than 30%.

Figure 2 shows the calculated profiles of the distribution of elastic stresses along the depth ε(z) for MBL with different types of the composition gradient. It should be noted that dependences ε(z) are similar for all types of MBL constructions considered in this work, unlike dependences ρ(z) that are strongly different from each other. The negative sign of ε demonstrates that only compression stresses take place in all these MBLs. In this case, the elastic stresses are quite low and are slightly changed in the range (0.5 – 3) × 10^{-4} almost in all layer thicknesses, except for the d_{free} region. In the MD-free region, the elastic stresses increase sharply; in the case of the step MBC, they are constant to thickness d_{free} and equal to ~1.5 × 10^{-4}; at the same time, in MBLs with linear and root profiles of changing the composition, the elastic stresses linearly increase with the thickness, achieving values ~3.5 × 10^{-3}, ~3.1 × 10^{-3}, and ~2.5 × 10^{-3} in the near-surface regions of linear, piece-linear, and root MBLs, respectively. In spite of these differences, all the layers are characterized by close values of integral $\int_{L-d_{free}}^{L} \varepsilon dz$. Thus, there are no substantial differences between different MBL constructions from the point of view of the compensation of residual stresses during subsequent growth of heterostructures on them.

The analysis shows that MBL with a root profile of changing the composition is the best construction of the buffer layer, in which the main MD density is concentrated in the lower part of MBL that is closer to the GaAs substrate. Note that such configuration of MD must lead to a decrease in the threading dislocation density, which we observed experimentally before [16].

Now we consider how the MD density distribution will be changed in this MBL construction in the dependence on the maximum In content and the layer thickness. Figure 3 shows the profiles of the MD density distribution in depth ρ(z) obtained for the root MBL with different x_{max}, assuming that, in all the cases, the compositions are changed with thickness $x(z)$ by the same law (the inset in Fig. 3). As seen from Fig. 3, the quite significant changes in the maximum In content in the root MBL from 75% to 87% almost do not influence the MD density distribution with

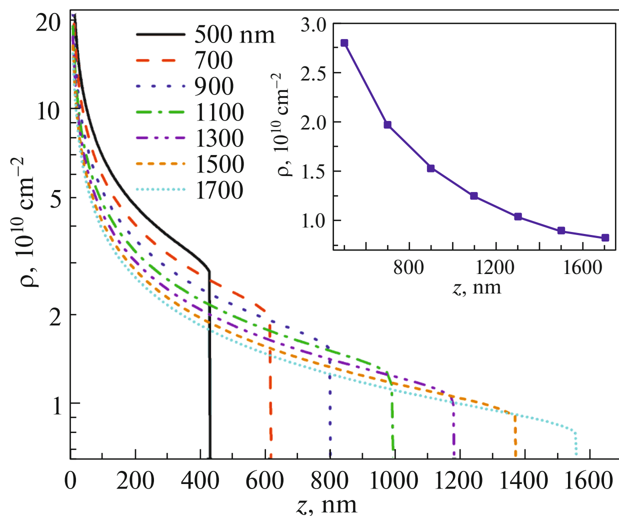

Fig. 4. Calculated coordinate dependences of the MD density along the growth direction obtained for the root $In_xAl_{1-x}As$ MBL ($x = 0.05$–0.87) of various thicknesses ($L = 500$–1700 nm). The inset shows dependence $\rho_0(L)$.

thickness and only insignificantly decrease ρ_0 in the upper part of the MBL from 1.1×10^{10} to 9×10^9 cm^{-2} and also increases the d_{free} region from 110 to 125 nm. It should be noted that these changes in ρ_0 and d_{free} are caused rather not so much by a change in the composition as by a change in the MBL thickness. This fact is confirmed by the calculations of dependence $\rho(z)$ for the root MBLs with different layer thicknesses but a fixed range of the composition change; the calculation results are given in Fig. 4.

As indicated in Fig. 4, the MD density distribution in the root MBL has inhomogeneous character at all, even at relatively small thicknesses. In spite of the fact that the MD density in the upper part of the MBL immediately adjacent to the d_{free} region is nonlinearly dependent on the layer thickness (dependence $\rho_0(L)$ in the inset in Fig. 4), the value of ρ is not higher than 3×10^{10} cm^{-2} even at small $L = 500$ nm. Thus, we can assume that the root MBL with a thickness halved as compared to thicknesses (1000–1500 nm) commonly used in traditional MBL constructions will not be inferior to them in crystallographic perfection and the threading dislocation density. This circumstance is doubtlessly important for practical realization of methamorphic heterostructures.

It should be noted that the simplified approach used in this work for calculating the MD density and residual stresses in MBL does not take into account the effect of interaction of dislocations to each other. This effect can substantially influence the distribution of the MD and TD densities and their decrease. Nevertheless, such calculations, as shown above, enable us to correctly predict the features in the distributions of the MD density and elastic stresses in different types of MBL and can be efficiently used when designing device methamorphic heterostructures.

4. CONCLUSIONS

We calculated the equilibrium distributions of the MD density $\rho(z)$ and elastic stresses $\varepsilon(z)$ along the epitaxial growth direction for $In_xAl_{1-x}As$ MBL with high In contents (to 87 mol %) and different types of the composition gradients: step, linear (piece-linear), and root. These MBL constructions strongly differ to each other in the character of distributions $\rho(z)$, while dependences $\varepsilon(z)$ are similar and the differences are observed only in the d_{free} region. In the root MBL, dependence $\rho(z)$ is rigidly nonlinear, unlike the traditional (step and linear) MBL with almost homogeneous MD distributions; in this case, the main part of MD is concentrated in the lower MBL part near the heteroboundary with a GaAs substrate. Note that we observed the noted feature experimentally before. In addition, it is found that the root MBL has the MD density in the upper part of the layer up to $\rho_0 \sim 9 \times 10^9$ cm^{-2} that is the lowest density among those of all the constructions and the highest thickness of the dislocation-free region $d_{free} = 125$ nm. It should be noted that, although dependences $\varepsilon(z)$ are different for various MBLs in the d_{free} region, the integral values of residual stresses in the dislocation-free regions for them are almost the same demonstrating that there are no substantial differences between different MBL constructions from the point of view of the compensation of residual stresses during subsequent growth of heterostructures on MBLs. The numerical method used for the calculation in this work, does not take into account the effect of interaction of dislocations to each other that leads to a decrease in the absolute TD density. Nevertheless, this method enabled us to qualitatively reproduce all the features of the MD density in different MBLs observed experimentally and to establish the characters of the distributions of elastic stresses in them. Therefore, this approach can be efficiently used when designing the optimal constructions of apparatus metamorphic heterostructures of various maximum compositions and required thickness.

FUNDING

This work was supported in part by the Russian Foundation for Basic Research, project no. 18-02-00950.

CONFLICT OF INTEREST

The authors declare that they have no conflicts of interest.

REFERENCES

1. G. B. Galiev, I. S. Vasil'evskii, S. S. Pushkarev, E. A. Klimov, R. M. Imamov, P. A. Buffat, B. Dwir, and E. I. Suvorov, J. Cryst. Growth **366**, 55 (2013).

2. W. Hafez, J. Lai, and M. Feng, Electron. Lett. **39**, 1447 (2003).
3. G. Belenky, D. Wang, Y. Lin, D. Donetsky, G. Kipshidze, L. Shterengas, D. Westerfeld, W. L. Sarney, and S. Svensso, Appl. Phys. Lett. **102**, 111108 (2013).
4. S. V. Ivanov, M. Yu. Chernov, V. A. Solov'ev, P. N. Brunkov, D. D. Firsov, and O. S. Komkov, Prog. Cryst. Growth Charact. Mater. **65**, 20 (2019).
5. V. A. Kulbachinskii, L. N. Oveshnikov, R. A. Lunin, N. A. Yuzeeva, G. B. Galiev, E. A. Klimov, S. S. Pushkarev, and P. P. Maltsev, Semiconductors **49**, 921 (2015).
6. D. J. Dunstan, P. Kidd, L. K. Howard, and R. H. Dixon, Appl. Phys. Lett. **59**, 3390 (1991).
7. D. J. Dunstan, J. Mater. Sci. Mater. Electron. **8**, 337 (1997).
8. H. Choi, Y. Jeong, J. Cho, and M. H. Jeon, J. Cryst. Growth **311**, 1091 (2009).
9. M. Yu. Chernov, V. A. Solov'ev, O. S. Komkov, D. D. Firsov, B. Ya. Meltser, M. A. Yagovkina, M. V. Baidakova, P. S. Kop'ev, and S. V. Ivanov, Appl. Phys. Express **10**, 121201 (2017).
10. B. Bertoli, E. N. Suarez, J. E. Ayers, and F. C. Jain, J. Appl. Phys. **106**, 073519 (2009).
11. S. Adachi, *Properties of Semiconductor Alloys: Group-IV, III-V and II-VI Semiconductors* (Wiley—Blackwell, 2009).
12. E. A. Fitzgerald, Mater. Sci. Rep. **7**, 87 (1991).
13. J. Zou, D. J. H. Cockayne, and B. F. Usher, J. Appl. Phys. **73**, 619 (1993).
14. I. N. Trunkin, M. Yu. Presniakov, and A. L. Vasiliev, Crystallogr. Rep. **62**, 265 (2017).
15. F. Capotondi, G. Biasiol, D. Ercolani, V. Grillo, E. Carlino, F. Romanato, and L. Sorba, Thin Solid Films **484**, 400 (2005).
16. V. A. Solov'ev, M. Yu. Chernov, A. A. Sitnikova, P. N. Brunkov, B. Ya. Meltser, and S. V. Ivanov, Semiconductors **52**, 120 (2018).

Translated by Yu. Ryzhkov